JOURNAL OF CATALYSIS **124,** 441–450 (1990)

Reactivity of Surface Species on Zeolites in Methanol Conversion

LUDMILA KUBELKOVÁ, JANA NOVÁKOVÁ, AND KVĚTA NEDOMOVÁ

The J. Heyrovsky Institute of Physical Chemistry and Electrochemistry,
Dolejskova 3, 182 23 Prague 8, Czechoslovakia

Received September 15, 1989; revised version received January 3, 1990

The surface species formed by the interaction of methanol with HY and HZSM-5 zeolites modified with nonskeletal Al were examined using FT-IR spectroscopy and temperature-programmed desorption accompanied by conversion of preadsorbed methanol with mass spectrometric detection of the products evolved. Physisorbed methanol perturbed by various surface sites, methylcarboxonium ions, skeletal methoxyls $\geqslant SiO(CH_3)Al \leqslant$, methoxyls on nonskeletal aluminium $Al_nO(CH_3)$, and methoxyls substituting for silanol groups $\geqslant SiO(CH_3)$ were found on both zeolite types. Their occurrence depended on the zeolite composition and the reaction temperature. The role of skeletal methoxyls and Al_nOCH_3 in the methanol conversion is discussed. In addition to the reaction of preadsorbed methanol the conversion over ZSM-5 catalysts under on-stream conditions was found to be sensitive to the presence of nonskeletal Al_n.

INTRODUCTION

Numerous mechanisms proposed by various authors to explain primary C–C bond formation in methanol conversion over acidic forms of zeolites involve the assumption of oxonium ions or carbenoid, ylide, or free radical reaction intermediates (*1–12*). The existence of these species, however, has not been demonstrated. Experimental evidence has been given only for methoxyls (*3–8, 13, 14*), formiates (*3, 7, 15*), and carbonates (*3, 7, 15*). The formation of protonated methanol was described in the heteropolyacid–methanol system (*16*); in zeolites, to date, only the protonated form of dimethylether (DME) has been found (*8*) after interaction with HZSM-5.

In this paper we concentrated on (i) methanol physisorption and the formation of its protonated form and (ii) various types of methoxyls and their possible role in the methanol reaction. This approach was adopted because methoxyls can act as precursors of carbene or ylide intermediates (*1, 3, 4, 7, 8, 10, 11, 17*). The discussion of the formation of surface complexes and their reactivity is based on the examination of Y and ZSM-5 zeolites with various compositions using Fourier-transform infrared spectroscopy (FT-IR) for the determination of surface complexes and mass spectrometric (MS) analysis of the products evolved during temperature-programmed desorption accompanied by conversion (TPDC) of preadsorbed methanol. The results of our previous TPDC-MS studies of methanol and hydrocarbon reaction with a methylated zeolite surface (*7, 17*) and of the effect of nonskeletal Al species in the Y zeolite on the amount and composition of the evolved products (*12*) are also employed for this purpose. To show the significance of nonskeletal Al species in the TPDC regime and elsewhere, the ZSM-5-methanol systems were also studied under on-stream conditions at atmospheric pressure and 400°C.

EXPERIMENTAL

The Y and ZSM-5 zeolites used in this study are listed in Table 1, where the silicon-to-aluminium ratios in the skeleton and in the whole zeolite are given. The next columns show the sorption capacity values, measured using Ar at −195°C and 13.3 kPa, and the positions and assignments of the IR bands of the hydroxyls in the original samples before methanol adsorption.

0021-9517/90 $3.00

TABLE 1

Characterization of Zeolites

No.	Zeolite	$(Si/Al)_t$	$(Si/Al)_s$	Capacity (mmol Ar g^{-1})	OH bands (cm^{-1})		
					SiOH	AlOH	SiOHAl
1	$H_{70}Na_{30}$-Y	2.50	2.5	10.9	3745	—	3644, 3548
2	AlH-Y	2.32	2.9	9.0	3745	—	3635, 3542
3	stab.Y	2.90	11.6	8.9	3745 3740	—	3631,[a] —
4	HZSM-5/a	19.0	19.0	5.6	3748	3664[a]	3611
5	HZSM-5/b	17.5	17.5	5.0	3745	3664[a]	3611
6	AlHZSM-5	16.0	19.0	5.5	3745	3664[a]	3611
7	HZSM-5 · Al_2O_3	5.8	19.0	5.1	3745 3720	3664	3611
8	NaZSM-5	19.0	19.0	5.6	3745	—	—

Note. t, Total; s, skeleton.

[a] Relatively very weak bands.

The $H_{70}Na_{30}$-Y, HZSM-5/a, and HZSM-5/b samples were supplied by the Research Institute for Oil and Hydrocarbon Gases, Czechoslovakia, in either their ammonium (Y and ZSM-5/b) or acidic (ZSM-5/a) forms. $AlNH_4$-Y and $AlNH_4$ZSM-5 zeolites containing cationic Al were prepared (*18*) by ion exchange of the original samples in ammonium form with 0.1 *M* $Al(NO_3)_3$ at 60°C and pH 4; sample 3 was obtained from $(NH_4)_{95}Na_5$-Y using hydrothermal treatment at 770°C in a steam and sample 7 from HZSM-5 (acid leached) by impregnation (*19*): HZSM-5 was first dehydrated under vacuum at 200°C, cooled to 60°C, and contacted with aqueous solution of $Al(NO_3)_3$ to incipient wetness under a nitrogen atmosphere. Nitrates were decomposed in an oxygen stream at 520°C. NaZSM-5 (sample 8) was prepared according to the method described in patent 20, example No. 27; organic salts were decomposed in an oxygen stream at 520°C.

Before interaction with methanol in IR and TPDC experiments, all the samples were treated *in situ* under vacuum at 400°C for 16 h, which resulted in elimination of water and ammonia and almost no dehydroxylation of the bridging OHs. Prior to catalytic experiments under on-stream conditions, the samples were activated *in situ* in a dry nitrogen stream at 450°C for 2 h.

The IR spectra of thin self-supported zeolite platelets (thickness 7 mg cm^{-2}) in an IR vacuum cell were recorded with a Nicolet MX-1E Fourier-transform spectrometer. Methanol was adsorbed at room temperature in an amount of 3.5 mmol g^{-1}; then the temperature was increased continuously (6°C min^{-1}) to 100, 180, 310, and 420°C with simultaneous evacuation of the cell (set A). After reaching the above temperatures, the sample was rapidly cooled and its spectrum was recorded. The composition of the gas phase was checked using MS in an off-line arrangement. Another set of experiments (B) consists of heating the sample at 130°C in methanol vapors at a pressure of 6 kPa and desorption of surface complexes at 200 and 360°C for 30 min, followed by cooling to room temperature and spectrum recording. Products evolved during continuous TPDC were directly analyzed by a Finnigan 400 quadrupole mass spectrometer. Methanol (0.3 mmol g^{-1}) was preadsorbed on the zeolite (0.1 g) at 25°C and desorbed with a heating rate of 6°C min^{-1}.

The experiments at atmospheric pressure were performed (*21*) with 24 vol% of methanol in a He stream using on-line gas chromatographic analysis of the products. The catalyst was in the form of 200-mg pellets, the reaction temperature was 400°C, and WHSV was 4 h^{-1}.

RESULTS AND DISCUSSION

Sample Characterization

Table 1 and Figs. 1, 3, and 4 show how the number of nonskeletal Al species and the number of individual types of hydroxyls vary in the studied Y and ZSM-5 zeolites. It can be seen that the nonskeletal Al content increases in the following sequence: HY < AlHY < stab.Y, and HZSM-5 < AlHZSM-5 < HZSM-5. Al_2O_3 (it is very small in the H forms (*12, 18*)). The number of skeletal bridging hydroxyls, $\geqslant$SiOHAl$\leqslant$, decreases in the reverse sequence, is very low in stab.Y, and drops approximately to $\frac{1}{5}$ of the initial value after impregnation of HZSM-5 with Al_2O_3. Some Al species designated as Al_2O_3 in this sample therefore act to compensate the charge on the skeleton.

Skeletal hydroxyls located in large and small cages of Y zeolites vibrate within the intervals 3644–3631 and 3548–3542 cm^{-1}, respectively, and the skeletal hydroxyls of ZSM-5 at 3611 cm^{-1} (Table 1). Nonskeletal Al species exhibit electron-accepting strong Lewis acid properties (*18*) and, in some cases, are also present as Al_nOH groups (band at 3664 cm^{-1}, Table 1). The SiOH groups on silica or silica-alumina impurities, on structure defects, or on the outer surface are present in all the samples studied, which is reflected in band(s) near 3745 cm^{-1} (Table 1) mostly with very low intensity (Figs. 1, 3, 4).

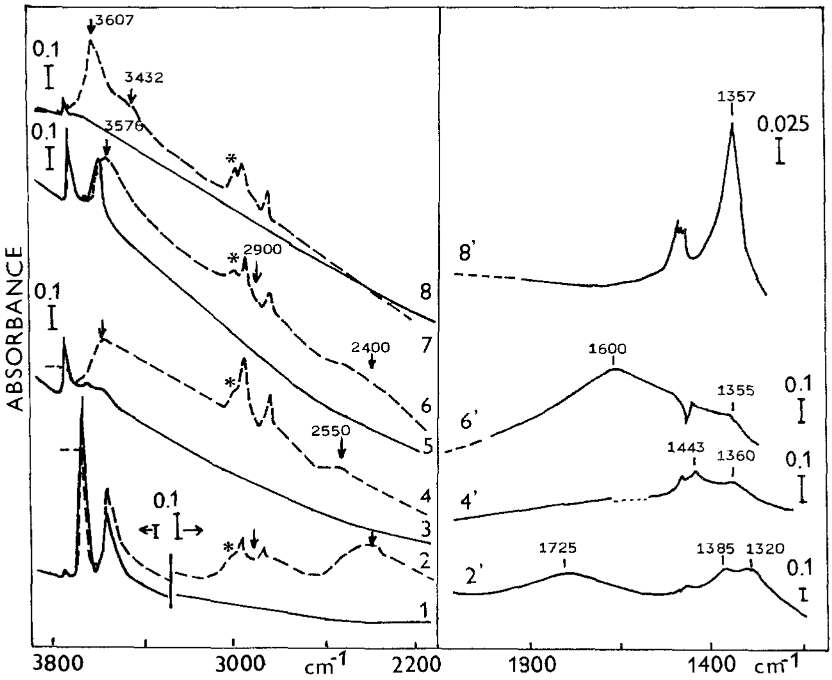

FIG. 1. IR spectra of the original HY, stab.Y, HZSM-5/b, and NaZSM-5 zeolites before (1, 3, 5, and 7, respectively) and after the adsorption of approximately 1 mmol g^{-1} of methanol at 25°C (2, 4, 6, and 8, respectively). Curves 2′, 4′, 6′, and 8′: spectra of pure surface species obtained by the subtraction of the zeolite spectrum from the spectrum of the whole system.

Complexes Adsorbed at Room Temperature

The infrared spectra of zeolites before and after the adsorption of approximately 1 mmol g^{-1} of methanol and those of the adsorbed species alone are depicted in Fig. 1. The assignment of the OH and CH_3 vibrational bands to the proposed methanol complexes is given in Tables 2 and 3, respectively.

The spectra show that the interaction of methanol with Na^+ ions leads to a slight weakening of the methanol OH bond. The new OH band appears at 3607 cm^{-1}, so that its shift of 75 cm^{-1} toward lower wave numbers with respect to the frequency of the OH vibration of gaseous methanol is far less than the value of 190 cm^{-1} reported for the methanol dimer (*23*) (Table 2). In contrast to Na^+, nonskeletal Al species, which are of a heterogeneous nature (*18*), cause rather wide perturbation of the methanol hydroxyls manifested in a flat, very broad band from 3570 to 2800 cm^{-1} (Fig. 1, stab.Y). The two bands of the methanol OH bending vibration found at 1360 and 1443 cm^{-1} for methanol adsorption on stab.Y and the single band at 1357 for methanol adsorption on NaZSM-5 support this interpretation.

Adsorption of CH_3OH on skeletal OH groups of acidic forms of zeolites (both HY and HZSM-5) results in the appearance of broad bands at approximately 3575, 2900, 2500–2400, and 1700–1600 cm^{-1}. These bands were also observed after the adsorption of CD_3OH. Because they are seen in

TABLE 2

Assignment of the OH Bands of Adsorbed Methanol

Methanol	Band (cm^{-1})	Vibrational mode	Complex
Gas[a]	3682	Stretching	—
	1346	Bending	
Dimer[b]	3490	Stretching	—
Liquid[a]	3337	Stretching	—
	1420	Bending	—
Adsorbed	3607 3432 sh	Stretching	$CH_3\overset{\overset{H}{\vert}}{O}..Na^+$
	1357	Bending	
	3570–2800	Stretching	$CH_3\overset{\overset{H}{\vert}}{O}..Al_n$, $CH_3\overset{\overset{H..O}{\vert}}{O}..Al_n$
	1443, 1360	Bending	
	3576	Stretching (methanol OH)	$CH_3\overset{\overset{H}{\vert}}{O}..H\underset{Al}{\overset{Si}{O}}$
	2900–2800	Stretching (skeletal OH)	
	1420–1360	Bending (methanol OH)	
	1320	2× out of plane (methanol OH)	
	3576	Stretching	$CH_3\overset{\overset{H}{\vert}}{O}H^+..{}^-\underset{Al}{\overset{Si}{O}}$
	2550–2400	Stretching	
	1720–1610	Bending	

[a] Ref. (*22*).
[b] Ref. (*23*).

TABLE 3

Assignment of CH_3 Vibration Bands (Observed in this Study)

Species	Specification	CH_3 vibration (cm^{-1})									Ref.[a]
		ass or ov, comb.	ass	ov, comb.	ss	Deformation					
CH_3OH^b	Gas		2977		2844		—	1477,		1455,	1415	*22*
	Liquid		2934		2822		—	1480,		1455,	1420	*22*
	Vitreous	2982	2951		2828				1452,	1415	*22*
$CH_3\overset{H}{O}..Na^+$	Adsorbed on: ZSM-5, Y	2990	2959	(2938)	2854		—	1477, 1464,	1455,	—	*8, 24*
$CH_3\overset{H}{O}..HO\genfrac{}{}{0pt}{}{Si}{Al}$	ZSM-5, Y ZSM-5, Y	3008	2961–2958	(2920)	2858–2852		—	1475, 1458–	1454	—	—
$(CH_3OH_2)^+$	ZSM-5, Y										
$CH_3\overset{H}{O}..Al_n$	ZSM-5, Y	3000	2966–2961	(2920)	2858–2855		—	1470, 1460,	—	—	—
CH_3OSi	SiO_2, ZSM-5, Y	3000–2996	2961–2958	2927 2987	2861–2858	1485,	—	1465,	—	—	*25–27*
$CH_3\overset{Si}{\underset{Al}{O}}$	ZSM-5, Y		2980–2977		2871		—	1468, 1459,	—	—	*3, 6–8, 13, 28*
CH_3OAl_n	ZSM-5, Y		2970–2968		2868	1490,	1472,	—	—	(1420)	*6*

Note. ass, Assymetric stretching mode; ss, symmetric stretching mode; ov, overtone; comb., combination tone; n, nonskeletal; values in parentheses are relatively very weak intensities.

[a] References describing analogical compounds.

[b] From the literature.

the spectra at very low coverages, we assigned them to the OH vibrations of the methanol which is hydrogen-bonded to the skeletal hydroxyls and of the methyl carboxonium ion $CH_3OH_2^+$ formed by the attraction of the skeletal proton. Details are given in Table 2. Note that methanol physisorption on the nonacidic SiOH of silica gel gives rise to a perturbed hydroxyl band (*25*, *26*) between 3500 and 3350 cm^{-1}. For the CH_3 vibrations, a well-developed shoulder on the high-frequency side of the most intense asymmetric stretching band of the CH_3 group (Table 3; marked with an asterisk in Fig. 1) allows us to assume an "unsymmetrical" form of the adsorbed methanol. Similar assignment of this shoulder was already published (*22*) for methanol molecules in C_s symmetry. The position of this shoulder appeared to be sensitive to the nature of the active sites: 2990, 3000, and 3008 cm^{-1} correspond to the methanol adsorbed on Na^+, nonskeletal Al, and skeletal hydroxyls, respectively.

Surface Methoxyls

The TPDC curves obtained in continuous MS experiments with Y zeolites are shown in Fig. 2, where arrows designate the temperature of the interruption of comparable experiments carried out to measure the surface complexes and the OH groups (Fig. 3). The spectra of surface species on ZSM-5 found in the course of set B experiments are given in Fig. 4 and the assignments of the most characteristic bands of the individual types of surface methoxyls, which are based on the comparison of the IR spectra obtained during TPDC runs on zeolites of various compositions, are given in Table 3.

For the HY zeolite, a small amount of adsorbed methanol remains in the cavities after reaching 180°C when the methoxy groups formed on the skeleton at even lower temperatures (*3*, *6*) (from about 100°C), most probably via methyloxonium ions, become the predominating surface complex:

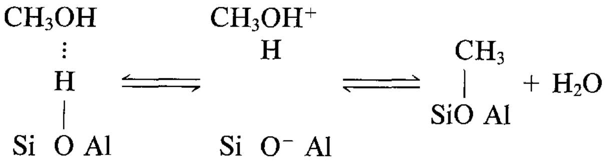

$$\begin{array}{c} CH_3OH \\ \vdots \\ H \\ | \\ Si\ O\ Al \end{array} \rightleftharpoons \begin{array}{c} CH_3OH^+ \\ H \\ \\ \\ Si\ O^-\ Al \end{array} \rightleftharpoons \begin{array}{c} CH_3 \\ | \\ SiO\ Al \end{array} + H_2O \qquad (1)$$

This follows from: (i) small bands at 2952 and 2850 cm^{-1} of the CH_3 groups and weak broad bands in the region 2900–2400 cm^{-1} of OH groups, indicating adsorbed methanol; (ii) pronounced bands at 2977 and 2871 cm^{-1} of the skeletal methoxyls; and (iii) intensity changes of band at 3644 cm^{-1} of free bridging hydroxyls (Fig. 3). The formation of DME above 180°C (Fig. 2) is accompanied by some lowering in the intensity of the skeletal methoxyl bands and a further lowering in the intensity of the bands of adsorbed methanol. Decomposition of remaining skeletal methoxyls (Figs. 2 and 3), however, readily occurs above 420°C. Note that skeletal methoxyls substitute ca. 20% of the skeletal hydroxyls in the large cavities. The frequencies of the skeletal methoxyl vibrations agree well with the values published in the literature (Table 3). Moreover, the presence of only very small wings on both sides of the 2977 cm^{-1} band can be interpreted as being a consequence of a "symmetric" CH_3O arrangement (for instance C_{3v}).

The spectra of the surface complexes on AlHY and stab.Y are clearly different from the spectra of complexes on HY. The new bands (see Table 3 and Fig. 3; the most characteristic band appears at 2970 cm^{-1}) are assigned to the $CH_3O–Al_n$ methoxy groups on the nonskeletal Al species which can be formed by the following reactions:

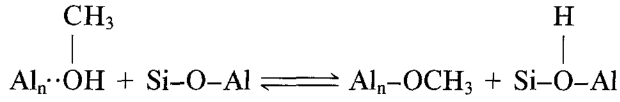

$$\begin{array}{c} CH_3 \\ | \\ Al_n\cdot\cdot OH \end{array} + Si–O–Al \rightleftharpoons Al_n–OCH_3 + \begin{array}{c} H \\ | \\ Si–O–Al \end{array} \qquad (2)$$

$$Al_nOH + CH_3OH \rightleftharpoons Al_n–OCH_3 + H_2O \qquad (3)$$

The reverse reactions and methanol more firmly bound to Al Lewis sites than to bridging hydroxyls are probably responsible for the shifts in the maxima of methanol desorption from AlHY and stab.Y to higher temperatures (Fig. 2, 220 and 280°C, respectively) compared with the desorption from HY (150°C).

Al_nOCH_3 complexes are present on both AlHY and stab.Y at 180°C together with adsorbed methanol. The concentration of these compounds appreciably decreases if the desorption temperature increases up to 310°C. Then Al_nOCH_3 predominates on stab.Y which contained very few bridging hydroxyls in the original form. With AlHY, however, the bands of skeletal methoxyls become evident in the vicinity of the bands of Al_nOCH_3. Further heating up to 420°C reduces the content of Al_nOCH_3 on both zeolites and also of skeletal methoxyls on AlHY. This also follows from the intensity decrease of the methoxyl bands and the intensity increase of the free bridging hydroxyls (Fig. 3). Because the TPDC curves indicate that, in contrast to HY zeolites, the hydrocarbons are formed in this latter temperature interval, the Al_nOCH_3 complexes can be considered to enhance the C–C bond formation and, possibly, also further consecutive reactions.

The spectra in Fig. 4 demonstrate that

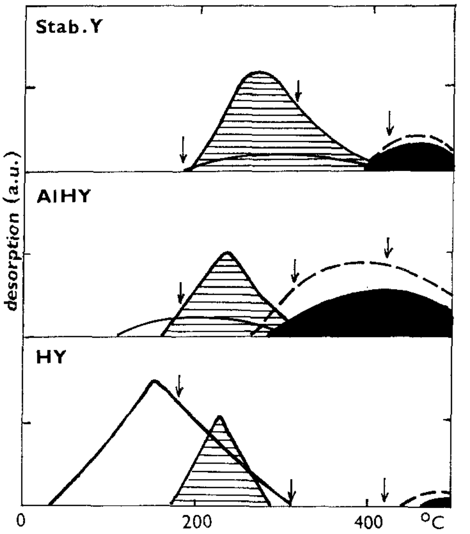

FIG. 2. TPDC of methanol and its reaction products from HY, AlHY, and stab.Y zeolites. (□) CH_3OH, (▤) $(CH_3)_2O$, (⬚) aliphatics C_2–C_5, (■) aromatics C_7–C_{10}.

ZSM-5 zeolites at 200°C contain skeletal methoxyls, Al_nOCH_3, and adsorbed methanol. The Al_nOCH_3 surface compounds were found even on nonmodified HZSM-5 (samples 4 and 5), which pyridine adsorption has shown to contain some Al Lewis sites. The intensity of the bands attributed to these methoxyls increases with the amount of nonskeletal Al on modified ZSM-5 (Fig. 4), which confirms the band assignment based on the experiments with various Y zeolites. A concentration decrease on heating to 420°C was found for all the surface complexes mentioned but the Al_nOCH_3 species were removed more readily than the skeletal methoxyls (Fig. 4). The TPDC experiments shown in Fig. 5 with HZSM-5 and HZSM-5 · Al_2O_3 again support the suggestion that the nonskeletal Al species improve the zeolite reactivity. Moreover, in

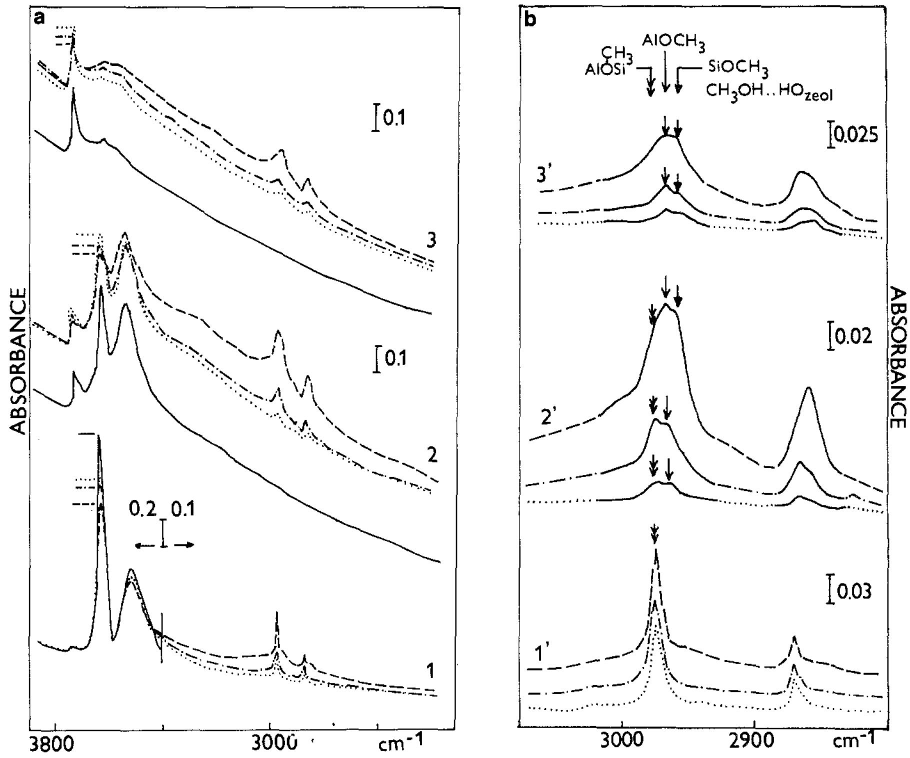

FIG. 3. IR spectra of HY (1), AlHY (2), and stab.Y (3) zeolites before (—) and during TPDC of methanol interrupted at 180°C (——), 310°C (–·–), and 420°C (...). Spectra designated by a number with a dash correspond to the spectra of surface species without zeolite bands.

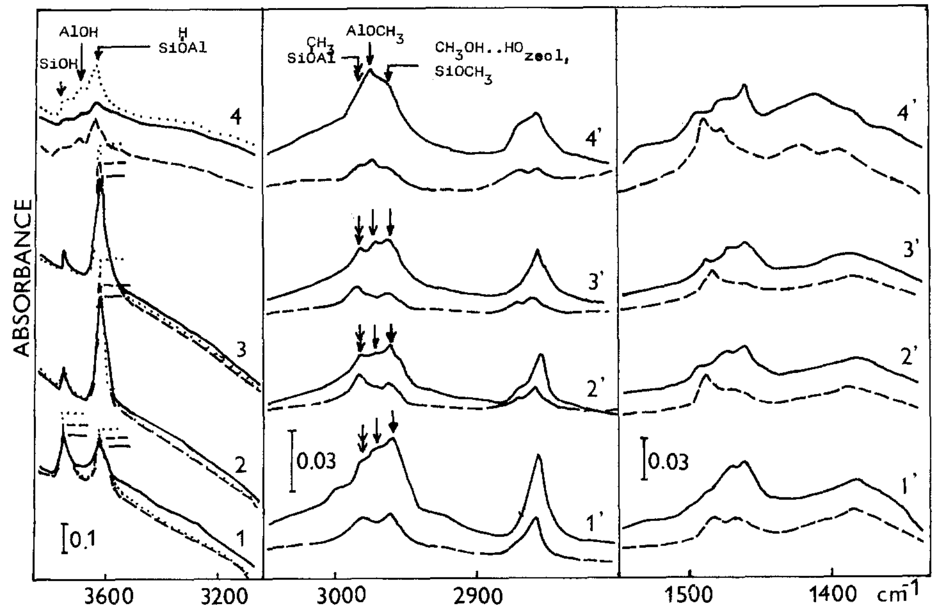

FIG. 4. IR spectra of HZSM-5/b (1), HZSM-5/a (2), AlHZSM-5 (3), and HZSM-5 · Al_2O_3 (4) before (...) and after the interaction with methanol at 135°C followed by the desorption at 200°C for 30 min (—) and 360°C for 30 min (– – –). Curves designated by a number with a dash correspond to the spectra of surface species without zeolite bands.

addition to higher hydrocarbons, the methane and formaldehyde were evolved from HZSM-5 · Al_2O_3.

The last type of methoxyls, $SiOCH_3$, substituting silanol groups, was always represented in the spectra by weak bands which were masked at the lower temperature of the desorption by the bands of adsorbed methanol (Table 3, most characteristic band at 2960 cm^{-1}). They were visible after the desorption at 420°C, namely for HZSM-5/b which contains the maximum of the SiOH groups (Fig. 4, curves 1′). For these reasons, the participance of $SiOCH_3$ complexes in the catalytic reaction cannot be discussed.

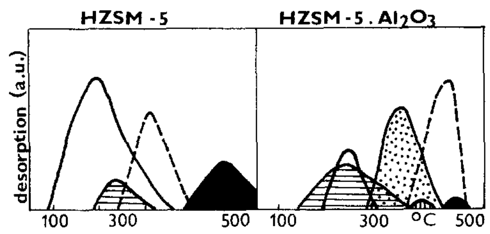

FIG. 5. TPDC of methanol and its reaction products from HZSM-5/a and HZSM-5 · Al_2O_3. (□) Methanol, (▤) dimethylether, (⬚) aliphatics C_2–C_5, (■) aromatics C_7–C_9, (▩) methane, and (▥) formaldehyde.

Comments on the Mechanism of Methanol Conversion

The ionic mechanism of methanol transformation usually includes methanol protonation in the first reaction step. The IR data presented here indicate the presence of a methyl carboxonium ion which is considered to be in equilibrium with adsorbed methanol H-bonded to the skeletal hydroxyls. Release of water above 100°C (1) is then accompanied by the formation of surface skeletal methoxyls which are known to exhibit appreciable methylating ability (*8*, *17*). In agreement with this, the spectral changes between 180 and 310°C when DME and methanol are evolved support the mechanism of DME formation (Figs. 2, 3, and, for instance, Ref. (*3*)) via the reaction of skeletal methoxyls (CH_3 as a whole) and the methanol molecule:

$$\geqq SiO(CH_3)Al \leqq + CH_3OH = \geqq AlOHSi \leqq + CH_3OCH_3 \quad (4)$$

Above 300°C, skeletal methoxyls are so highly reactive that they readily participate in the formation of C–C bonds. In contrast to the preceding case, the C–H bonds in the methyl group are now weakened (*29*) and hydrogen can be readily abstracted by the basic oxygens of the system. In this way, intermediates with ylide and carbene nature may be formed. The frequencies of the asymmetric stretching vibrations of the methyl groups were found to decrease in the following sequence: skeletal methoxyls > Al_nOCH_3 > $SiOCH_3$. Thus the C–H bonds in Al_nOCH_3 are weakened more than those in the skeletal methoxyls; this fact could explain the higher reactivity of zeolites with nonskeletal Al than zeolites in pure H form. Al_nOCH_3 is most probably also involved in the disproportionation of methoxyls yielding methane and formaldehyde under certain circumstances.

It was shown in the previous paper (*7*) that addition of methanol over the zeolite during TPDC above 300°C results in a strong increase in hydrocarbon formation. This effect can be a result of the basicity of methanol molecule which is higher than that of the zeolitic oxygens (the pK_a of the bridging hydroxyls (*30*) is <-8, while that (*31*) of $CH_3OH_2^+$ is -3.8), so that the methanol molecule is more active in the hydrogen abstraction from methoxyls than the zeolite oxygens. Methanol reformed from methoxyls at higher temperatures (Fig. 2, Eqs. (2) and (3)) thus can also be considered to improve the hydrocarbon formation during TPDC from zeolites containing nonskeletal Al.

The possibility of a radical route (*32*) should also not be excluded, although the questions of radical generation and their role are still open.

The enhancement of the HZSM-5 catalytic activity and the higher selectivity for aromatics caused by the addition of nonskeletal Al species were also found at the beginning of the catalytic run carried out at 400°C under on-stream conditions at atmospheric pressure. However, the nonskeletal Al species accelerate the deactivation of zeolites, as is demonstrated in Fig. 6. It is tempting to assume that the aldolization reactions of formaldehyde affect this process.

CONCLUSIONS

(i) Adsorption of methanol on skeletal hydroxyls results in the formation of a hydrogen-bonded complex which is in equilib-

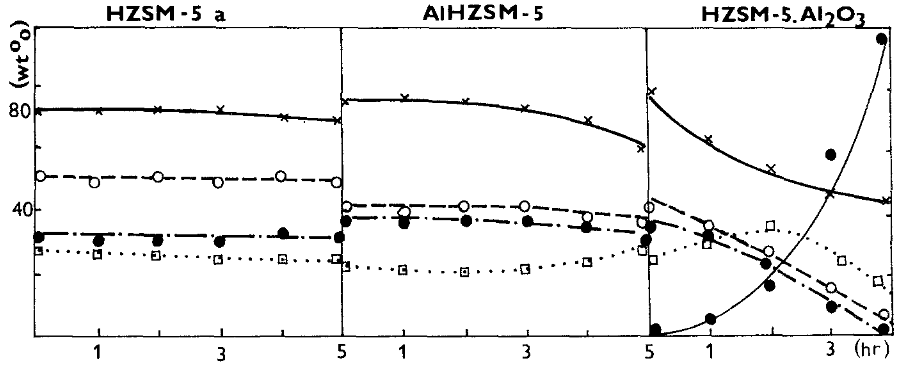

FIG. 6. Dependence of methanol conversion at 400°C and reaction selectivity over HZSM-5/a, AlHZSM-5, and HZSM-5 · Al_2O_3 on the time-on-stream. Conversion (-×-), selectivity for paraffins (–––), olefins (...), aromatics (–·–) and dimethylether (-●-).

rium with the monomethyl oxonium ion. Adsorption of a methanol molecule also occurs on electron-accepting $\mathrm{Al_n}$ sites. Further transformation to surface methoxyls readily proceeds above 100°C.

(ii) Above 180°C at least three types of methoxyls are present in the acid forms of the zeolites (Y, ZSM-5), i.e., on silica impurities or lattice defects, on nonskeletal Al species, and directly on the skeleton. The frequency of their asymmetric stretching CH_3 vibration and, consequently, the CH bond strength and positive charge on the methyl group decrease in the order: $\geqq\mathrm{AlOCH_3Si}\leqq\ >\ \mathrm{Al_nOCH_3}\ >\ =\!\mathrm{SiOCH_3}$.

(iii) $\mathrm{Al_n}$ and skeletal methoxyls participate in the formation of dimethylether by the reaction with methanol molecule at low temperatures. Above 300°C, the surface methoxyls, whose CH bonds are weakened, react to yield a primary C–C bond. Their reaction with methanol proceeds more readily then mutual reaction. The reactivity of the catalyst is especially increased if $\mathrm{Al_nOCH_3}$ groups are present together with skeletal methoxyls. The presence of the former groups is probably important for the occurrence of the disproportion yielding methane and formaldehyde over ZSM-5.

(iv) The presence of $\mathrm{Al_n}$ increases the activity of the catalyst at the beginning of the reaction under on-stream conditions but then leads to a more rapid deactivation.

REFERENCES

1. Chang, C. D., *ACS Symp. Ser.* **368,** 53 (1988); *Catal. Rev. Sci. Eng.* **25,** 1 (1983), and references therein.
2. Van den Berg, J. P., Wolthuizen, J., and van Hoof, J., *in* "Proceedings of the 5th International Conference on Zeolites" (L. V. C. Rees, Ed.), p. 649. Heyden, London, 1980.
3. Salvador, P., and Kladnig, W., *J. Chem. Soc. Faraday Trans. 1* **73,** 1153 (1977).
4. Ono, Y., and Mori, T., *J. Chem. Soc. Faraday Trans. 1* **77,** 2209 (1981).
5. Sayed, M. B., and Cooney, R. P., *Aust. J. Chem.* **35,** 2483 (1982).
6. Kubelková, L., Nováková, J., and Jírů, P., *in* "Structure and Reactivity of Modified Zeolites" (P. Jacobs *et al.,* Eds.), p. 217. Elsevier, Amsterdam, 1984.
7. Nováková, J., Kubelková, L., and Dolejšek, Z., *J. Catal.* **108,** 208 (1987).
8. Forester, T. R., and Howe, R. F., *J. Amer. Chem. Soc.* **109,** 5076 (1987).
9. Ison, A., and Gorte, R. J., *J. Catal.* **89,** 150 (1984).
10. Hutchings, G. J., Gottschalk, F., Hall, M. V., and Hunter, R., *J. Chem. Soc. Faraday Trans. 1* **83,** 571 (1987).
11. Kazansky, V. B., *React. Kinet. Catal. Lett.* **35,** 237 (1987).
12. Nováková, J., and Kubelková, L., *Catal. Lett.* **1,** 223 (1988).
13. Bosáček, V., and Tvarůžková, Z., *Coll. Czech. Chem. Commun.* **36,** 551 (1971).
14. Derouane, E. G., Gilson, J.-P., and Nagy, J. B., *Zeolites* **2,** 42 (1982).
15. Unland, M. L., *J. Phys. Chem.* **82,** 580 (1978).
16. Highfield, J. G., and Moffat, J. B., *J. Catal.* **95,** 108 (1985).
17. Nováková, J., Kubelková, L., and Dolejšek, Z., *J. Mol. Catal.* **45,** 365 (1988).
18. Kubelková, L., Beran, S., Malecka, A., and Mastikhin, V. M., *Zeolites* **9,** 12 (1989).
19. Kustov, L. M., Kazansky, V. B., Beran, S., Kubelková, L., and Jírů, P., *J. Phys. Chem.* **91,** 5247 (1987).
20. Agrauer, R. J., and Landolt, G. R., U.S. Patent 3702886 (1972).
21. Nedomová, K., Wichterlová, B., Beran, S., and Bednářová, S. *Catal. Today* **3,** 373 (1988).
22. Falk, M., and Whalley, E., *J. Chem. Phys.* **34,** 1554 (1961).
23. Inskeep, R. G., Keliker, J. M., McMahon, P. E., and Somers, B. G., *J. Chem. Phys.* **28,** 1033 (1958).
24. Kiselev, A. V., Lygin, V. I., and Starodubtseva, P. V., *Zh. Fiz. Khim.* **49,** 405 (1975).
25. Borello, E., Zecchina, A., and Morterra, C., *J. Phys. Chem.* **71,** 2938 (1967).
26. Kubelková, L., Schürer, P., and Jírů, P., *Surf. Sci.* **18,** 245 (1969).
27. Morrow, B. A., *J. Chem. Soc. Faraday Trans. 1* **70,** 1527 (1974).
28. Tvarůžková, Z., Tupá, M., Jírů, P., Nastro, A., Giordano, G., and Trifirò, F., *Catal. Lett.* **2,** 369 (1989).
29. Nováková, J., Kubelková, L., and Dolejšek, Z., *J. Catal.* **97,** 277 (1986).
30. Kubelková, L., Beran, S., and Lercher, J. A., *Zeolites* **9,** 539 (1989).
31. Noller, H., Mayerbok, B., and Zundel, G., *Surg. Sci.* **33,** 82 (1972).
32. Chang, C. D., Hellring, S. D., and Pearson, J. A., *J. Catal.* **115,** 282 (1989).